Chapter

Emerging Thin Film Solar Panels

Mahmoud Zendehdel, Narges Yaghoobi Nia
and Mohammadreza Yaghoubinia

Abstract

Utilizing of photovoltaics (PVs) has been rapidly developing over the past two decades due to its potential for transition from fossil fuels to renewable energy based economies. However, PVs as fuel less energy sources will be sustainable if some issues such as raw materials abundance, production cost, and environmental impacts carefully addressed in their value chains. Among PV technologies, thin film solar panels have been illustrated the potential to reach the sustainability. In this chapter we review some studies about environmental impacts of thin film PVs through life cycle assessment (LCA) and some environmental fate modeling. For the PV technologies, LCA studies need to be conducted to address environmental and energy impacts and encourage the development of PV technologies in a better sustainable way. Three methods of impact assessment in LCA are reviewed and compared, namely, Energy Payback Time (EPBT), Cumulative Energy Demand (CED), and Greenhouse Gases (GHG) emission rate, owing to data and information published in the literature. Generally, most results show promising potential of emerging thin film PVs, especially perovskite solar cells, to reach the best sustainable solution among PV technologies in near future.

Keywords: perovskite solar cell, life cycle assessment, emerging thin film photovoltaics, environmental impact, sustainable energy

1. Introduction

1.1 Sustainability of solar energy

The most requiring environmental concerns which need to be addressed are impacts of fossil fuels, Climate change, resource depletion, and worldwide energy shortage. The mentioned concerns will be more fundamental when we want to find the sustainable energy solutions for the future. Solar energy as the most abundant natural power resource on earth, can generate renewable energy by converting sunlight to thermal or electrical power by using of the photovoltaic (PV) devices. The effective solar irradiance which arrive the earth's surface varies between 125 and 305 Wm^{-2} by considering the latitude-dependent oblique incidence, diurnal variation, and seasonal variation. As it is known, solar energy is one of the continual power sources that could provide energy independence and energy security for all nations. At the moment, solar power is adopted as a substantial electricity generation in many developed and developing countries in order to address the energy demands. However, PVs as fuel-free energy sources inherently will be sustainable unless they are too expensive to produce, the materials needed for their production are depletable, or they create serious environmental impacts.

Net annual CO_2 emission mitigation potential from 1.8 kWp solar PV pump at an average solar radiation of 5.5 $kWhm^{-2}$ is about 2085 kg from diesel pumps and about 1860 kg from petrol pumps. An investigation on generation costs and carbon emissions of the conventional energy production technologies compared with solar power generation is presented in **Table 1** [1].

1.2 Photovoltaic technologies

The present PV technologies could be classified in two categories: (1) wafer-based (2) thin film cells (**Figure 1**). Wafer-based cells are fabricate on semi-conducting wafers and could be handled without an additional substrate, while modules are typically covered with glass for improving the mechanical stability and more protection. Thin film cells consist of semiconducting layers which can be deposited onto various substrates such as plastic, glass or metal. Further division of thin films into commercial and emerging thin film technologies is presented in **Figure 1**.

1.2.1 Wafer-based technologies

Three primary wafer-based technologies exist in the market containing: (1) Crystalline Silicon (c-Si), (2) Gallium Arsenide (GaAs) and (3) III-V multijunction (MJ). Among these types, c-Si PVs have occupied ~90% of present global manufacturing capacity and are the most mature of all PV technologies. Silicon solar cells are divided as single-crystalline (sc-Si) or multicrystalline (mc-Si). The sc-Si is typically fabricate through Czochralski (CZ) [3] or float-zone (FZ) methods, while mc-Si ingots are produced by casting technique. Usually, the fabricated ingots are sliced into 150–180 μm wafers prior to cell processing. High photoconversion efficiencies of sc-Si can be achieved by heterojunction with intrinsic thin layer (HIT) architecture, which consists of n-type sc-Si with thin amorphous silicon films. The mc-Si cells contain randomly oriented silicon grains with average size of 1 cm^2. Present record cell efficiencies stand at 27.6% for sc-Si and 22.3% for mc-Si [4]. Indirect bandgap of c-Si is one fundamental limitation, which leads to weak light absorption and needs wafer structures with ~100 μm thicknesses, excluding advanced light-trapping strategies. Key technological challenges for c-Si consist of stringent material purity requirements, large volume material utilization, restricted module form factor, and batch-based cell fabrication and module integration processes with relatively low throughput.

The GaAs is well suited for solar energy conversion, because of, a direct bandgap well matched to the solar spectrum, strong absorption and very low non-radiative energy loss. For lab cells the highest power conversion efficiencies of 30.5% has achieved by GaAs [4]. Flexible thin films of GaAs can be fabricated through epitaxial liftoff technique which can amortizes the substrate costs by recycling of GaAs wafers [5]. However this method has not yet been developed in high production scale. There are still some economical aspects such as, need to improve the film quality, more substrate recycling, and low-cost polishing of wafer, which need to be

Technology	Carbon emissions (gC/kWh)	Generation costs (USD/kWh)
Solar thermal and solar PV systems	0	9–40
Pulverized coal-natural gas turbine	100–230	5–7

Table 1.
Economic and emissions of conventional energy production technologies compared with solar power generation.

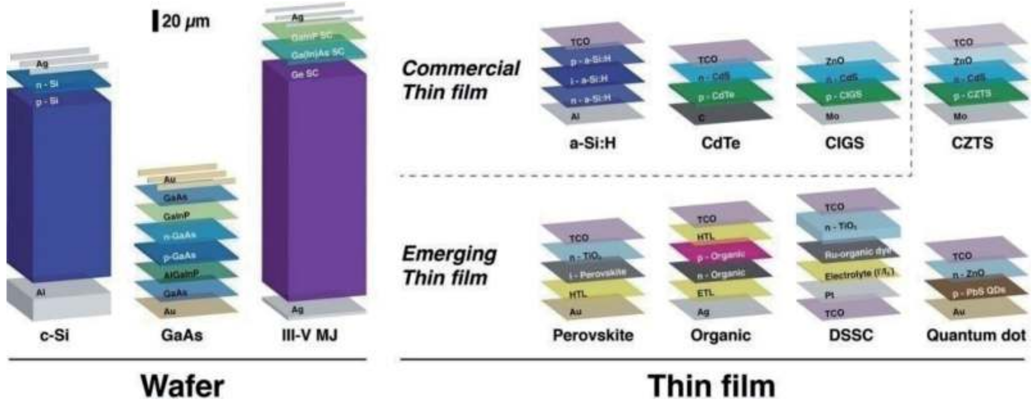

Figure 1.
Typical PV device structures, divided into thin film and wafer-based technologies. Primary absorber layers are labeled in white color, and thicknesses are shown to scale (obtained under copyright of Royal Society of Chemistry [2]).

addressed. In any case, high precursor costs may limit the large-scale development of such PV systems.

The III-V multijunction (MJ) solar cells stack of two or more single-junction cells with different band gaps which are used for absorbing of the solar irradiation with minimum thermalization losses. As it is known, semiconducting compounds of group V (N, P, As, Sb) and group III (Al, Ga, In) elements can form crystalline films with variable band energies, yielding unparalleled power conversion efficiencies, 35.5, 44.4, and 46.0% for record 4-junction (2 J), 3 J, and 4 J cells, respectively, under concentrated illumination [4]. One of the leading technologies for space application is III-V MJs, owing to their high radiation resistance, high efficiency and low temperature sensitivity. However, complex manufacturing processes in addition to high material costs make III-V MJ cells very expensive for large-area terrestrial applications.

1.2.2 Commercial thin-film PV

As it can be seen that c-Si currently dominates the global PV market, but alternative technologies may be able to reach lower costs in the long run. Solar cells based on thin semiconducting films constitute ~10% of global PV module market nowadays. Generally, thin-film cells are made by additive fabrication processes, which may reduce manufacturing capital expense and material usage. This category extends from commercial technologies based on conventional inorganic semiconductors to emerging technologies based on nanostructured materials. At the moment (2019), three thin film PV technologies which are developed to commercial phase are (1) hydrogenated amorphous silicon (a-Si:H), (2) cadmium telluride (CdTe) (3) copper indium gallium diselenide ($CuIn_xGa_{1-x}Se_2$, or CIGS).

Hydrogenated amorphous silicon (a-Si:H) offers higher absorption compare to c-Si, although having larger band gap respect to the c-Si (1.7–1.8 eV, compared to 1.12 eV for c-Si) is not well matched to the solar spectrum [6]. Amorphous silicon as a thin film PV is typically fabricated by plasma-enhanced chemical vapor deposition (PECVD) at relatively low substrate temperatures of 150–300°C. Since, only a 300 nm film of a-Si:H can absorb ~90% of above band gap photons in a single pass, this properties led to having lightweight and flexible solar cells and panels. Another properties of a-Si:H cell is that it can be combined with cells based on nanocrystalline silicon (nc-Si) or amorphous silicon-germanium (a-SiGe) alloys to form a multijunction cell without lattice-matching requirements. Nowadays most commercial a-Si:H modules use multijunction approach. As we know silicon is cheap, non-toxic and earth abundant, but while a-Si:H cells are well suited for small scale and low-power applications, their properties such as light induced degradation (the Staebler-Wronski effect [7]) and low efficiency compared to mature thin film technologies led to decreasing market interest.

Leading thin-film PV in the present global market is Cadmium telluride (CdTe). This type of PV is a favorable semiconductor for solar energy harvesting, via a direct band gap of 1.45 eV and strong solar spectrum absorption. CdTe has record efficiencies of 22.1% for the lab-scale cells and efficiencies of the commercial module continue to improve steadily [4]. CdTe technologies employ high throughput deposition processes and the lowest module costs of any PV technology on the market offered by CdTe technology, although relatively high processing temperatures are required (~500°C). However, one of the main concerns that have motivated research on alternative material systems is about the toxicity of elemental cadmium and the scarcity of tellurium.

Copper indium gallium diselenide (CIGS) is a semiconductor composite with a direct band gap of 1.1–1.2 eV. This class of thin film PVs can be fabricated by a variety of solution- and vapor-phase techniques from polyimide substrates or flexible metals [8], which make CIGS as a favorable PV for building-integrated and other unconventional PV applications. CIGS solar cells exhibit high radiation resistance which is mandatory for space applications. For the concentrator cells record efficiencies stand at 23.3% [4]. Some of Key technological challenges are listed as: (1) high variability in film stoichiometry and physical properties, (2) limited knowledge of the grain boundaries activity [9], (3) low open-circuit voltage due to structural and electronic inhomogeneity [10], (4) engineering of higher-band gap alloys to enable multijunction devices [11]. One reason could hinder large-scale deployment of CIGS technologies is the scarcity of indium element. The active materials which are used as light absorber in commercial thin-film PV technologies can absorb the sun light 10–100 times more efficiently than silicon, allowing use of films just a few microns thick. Low precursor materials use is thus a key advantage of these commercial thin film technologies which can affect on the LCA results as well.

1.2.3 Emerging thin-film PVs

Recently, several new thin-film PV technologies have emerged as a result of intense R&D efforts in materials discovery and device engineering. Key emerging thin-film PV technologies could be classified to 5 technologies consist of, (1) copper zinc tin sulfide (Cu_2ZnSnS_4, or CZTS), (2) perovskite solar cells (PSCs), (3) organic photovoltaics (OPV), (4) dye-sensitized solar cells (DSCs) (5) colloidal quantum dot photovoltaics (QDPV).

CZTS is an Earth-abundant alternative technology respect to CIGS, with similar processing challenges and strategies [12]. One of the important challenges consists of uncontrolled Cu and Zn inter-substitution which led to point defects, blocking charge extraction and reduce the open-circuit voltage of the cell [13]. Record certified cell efficiencies of CZTS cells have gained 12.6% [4].

Perovskite solar cells (PSCs) have been raised from solid-state dye-sensitized solar cells [14] and have quickly illustrated as one of the most promising emerging thin-film PV technologies, achieving the certified efficiencies of 24.2% [4] in 3 years of development in lab-scale devices. The term "perovskite" refers to the ABX3 crystal structure, and the most widely investigated perovskite for solar cells is the hybrid organic–inorganic lead halide (MA and/or FA)$Pb(I, Cl, Br)_3$. One of the interesting properties of perovskite structures is high band gap tunability in the range of 1.25–3 eV by substitution of cation or anion in the lattice (e.g., $HC(NH_2)_2Pb(I_{1-x}Br_x)_3$ [15], $CH_3NH_3SnI_3$ [16], and $CH_3NH_3Pb(I_{1-x}Br_x)_3$ [17]). Various low temperature techniques for the solution or vapor deposition can be successively utilized for fabrication the perovskite thin films [18, 19]. The important structural/physical properties of such hybrid perovskite layers could be classified as, long diffusion lengths of charge carriers [20], low recombination reaction [21], low cost precursor materials, and wide band gap tunability. Open circuit voltage (Voc) is one the most difficult parameters to improve in PV devices, while recently PSCs could achieved high Voc (more than 1.1 V). However, there are many issues which should be considered such as device life span, high sensitivity to the water, control the film morphology and reproducibility from batch to batch of fabrication, and present of toxic lead element.

As it is known in OPV generally organic small molecules [22] or polymers [23] are used for absorb the light. These materials have some specific properties such as using of earth abundant materials and easy scale-up the thin film structures by using of various deposition techniques [24]. Furthermore, fabrication of organic multijunction devices could be more economic in compare to the conventional III-V MJs due to high defect tolerance and leisure deposition routes [25]. At the moment the lab-made OPV cells could reach to 15.6% certified efficiencies [4]. Key concerns of these systems involve inefficient exciton transport [26], poor long-term stability [27], low large-area deposition yield, and low ultimate efficiency limits [28].

DSCs are among the most mature of nanomaterial-based PV technologies [29]. These photoelectrochemical cells consist of a transparent inorganic scaffold anode (typically nanoporous TiO_2 or other n-type oxides of transition metals) sensitized with light-absorbing dye molecules (ruthenium (Ru) complexes or organic dyes). Unlike the other solid-state technologies which are discussed here, DSCs often utilize a liquid electrolyte for transport ions to a counter electrode. DSCs have achieved efficiencies of up to 12.3% [30] and may benefit from low-cost materials, colorful and flexible modules and simple assembly. Main challenges of DSCs involve limited long-term stability under illumination and high temperatures, low absorption in the near-infrared, and low open-circuit voltages created from interfacial recombination.

QDPV technologies are improving consistently, with a record certified cell efficiency of 16.6% [4]. QDPV, also known as quantum dots (QDs), use solution-processed nanocrystals for absorb the sun light [31]. The ability to tune the band gap of colloidal metal chalcogenide nanocrystals (primarily PbS) by changing their size allows efficient harvesting of near-infrared photons, as well as the potential for multijunction cells using a single material system [32]. QDPVs have some advantages such as simple room-temperature fabrication and air-stable operation [33]. However, incomplete knowledge of surface chemistry and low open-circuit voltages that may be limited fundamentally by mid-gap states or inherent disorder in QD films make some challenges though development of these class of emerging PVs [34].

These emerging thin-film technologies employ nanostructured materials that can be engineered to achieve desired electronic and optical properties. Earth-abundant materials and relatively simple processing methods open a promising gate for large-scale manufacturing and deployment of such emerging PVs. However despite the unique device properties (e.g., transparency, light weight and flexibility) of these technologies, the maturity from R&D to industrial production and commercialization has not yet been developed. In any case, we believe that the mentioned emerging thin-films can solve many problems of present PV market due to their specific properties and ultra low production cost.

1.3 Life cycle assessment

Life Cycle Assessment (LCA) is a universal model for study the impacts of a system during its life cycle and production chain. This model is very useful method for evaluation of the environmental impacts, energy consumption and economical aspects of a system or product. In the LCA usually a "cradle-to-grave" or "cradle-to-gate" rough has been utilized for different steps in life cycle such as, raw material extraction, transport, processing, fabrication, distribution, utilization, and disposal aspects [35]. Owing to the standard protocol of ISO 14040 [36] and ISO 14044 [37], the LCA methodology consists of four distinct steps as shown in **Figure 2**.

1. Life Cycle Inventory (LCI): consist of data collection from the system (e.g., precursor materials, amounts of energy and water consumption, fabrication routes, waste treatment, products and environmental emission of by-products).

2. Life Cycle Impact Assessment (LCIA): Explain the potential environmental impacts, (e.g., eco-toxicity, ozone depletion, global warming and acidification).

3. Goal and scope definition: Determine the process roadmap, set the system's boundaries, define the functional unit, and formulate some assumptions.

4. Interpretation: conclude the LCI and LCIA results, analyze the critical points, and make recommendations for future improvements.

An effective LCA will quantify the technological, environmental, economic, and social aspects of a product/process that plays a fundamental role for reducing the life cycle impacts toward more sustainable options.

According to the Methodology Guidelines for the LCA of PV systems [38], the life cycle of a PV technology or product starts from the extraction of raw materials and ends with the disposal or recycling, as illustrated in **Figure 3**. During the

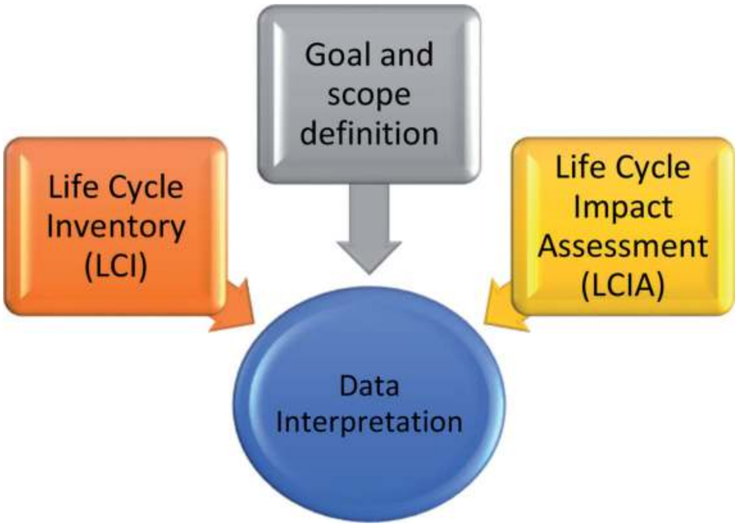

Figure 2.
General framework of life cycle assessment (LCA).

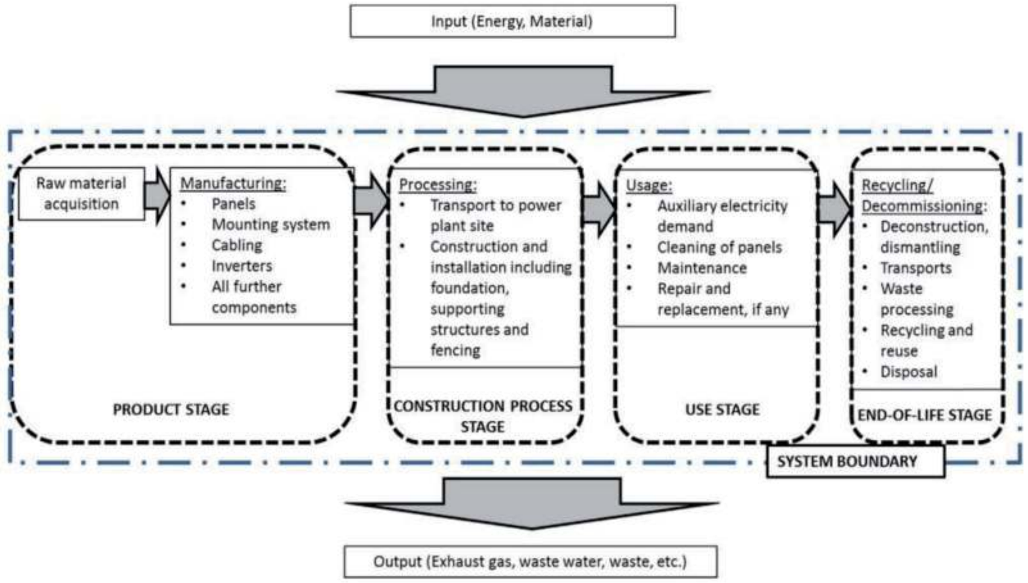

Figure 3.
The system boundary of solar PV life cycle (the figure is obtained under copyright of Elsevier [35]).

production section, insertion of raw materials, energy supply, manufacturing of panels, mounting system, cables, inverters, and all other components needed to produce electricity from sun light should be included in the system boundaries. Furthermore, some activities such as transportation, construction, and installation of the products, should be evaluated in the construction stage. In the utilization stage, some aspects, such as auxiliary electricity request, cleaning of the panels and maintenance of the plant should be included in the system boundaries. Finally, the recycling issues and waste treatments should be studied in the end-of-life stage.

Accordingly, the goal of this LCA is analysis the environmental impacts and other problems of PV systems during their life cycle which make a useful vehicle for improvement of each technology. Generally, this evaluation realizes three indicatives solar PV performance containing, Cumulative Energy Demand (CED), Energy Payback Time (EPBT), and GHG emission rate or Global Warming Potential (GWP). Those parameters are the most usable metrics applied in comparative life cycle evaluations of PV system.

The Cumulative Energy Demand (CED) is an energetic factor that quantifies the energy requirement during the life cycle of a product.

The Global Warming Potential (GWP) method, developed by the International Panel of Climate Change (IPCC), assesses the impact of the whole life cycle on global warming issue in terms of carbon dioxide (CO_2) emission.

The EPBT is an energetic indicator usually used for comparison of different energy production technologies, like PVs. It is represented in years and shows the needed time for generate the same amount of system's consumed energy in life cycle.

2. Life cycle assessment of thin film PVs

2.1 LCA of commercial thin film PVs

Environmental impacts of solar PV systems have been illuminated by several recent researches. Despite huge manufacturing of the crystalline silicon based PV systems, these generations of PVs have been shown higher environmental impact in comparison to thin film PVs. In particular, CdTe PV systems by presenting low life cycle impacts and low production costs compared with c-Si based PVs, can be considered as sustainable solution to the future Cd oversupply problem that has been projected in East Asia [39].

In a comparison between crystalline and amorphous silicon PVs (first and second PV generations), Pacca et al. [40] have been shown shorter EPBT values for a-Si (3.2 years) compare to mc-Si (7.5 years). In this study they assessed three LCA metrics, namely, Net Energy Ratio (NER), EPBT, and GHG emissions, on a 33-kW rooftop installation. However, if the photoconversion efficiency of cells can be increased in the future, the EPBT for a-Si and multi-Si could drop to 1.6 and 5.7 years, respectively. The GHG emission rate also exhibits the same pattern as EPBT, presenting lower values (34.3 g $CO_{2\text{-eq}}$/kWh) for a-Si in compare to mc-Si (72.4 g $CO_{2\text{-eq}}$/kWh). In another work, Minemoto et al. [41] have been reported the impact of solar spectrum distribution and module temperature on the outdoor performance of a-Si and mc-Si PV modules installed. Owing to their results, the output energy of a-Si modules mainly depends on spectrum distribution and is higher under blue-rich part of spectrum while that is less sensitive to module temperature.

The stages of the CdTe PV life cycle during thin film manufacturing has been reported by Fthenakis [42]. Firstly, Cd was extracted from zinc ores (~ 80%), while Te was prepared from Cu ores. Cd and Te were subsequently purified to more than 99.99% through electrolytic purification. Subsequently, a transparent conducting oxide (TCO) layer was deposited onto a glass substrate and a thin film of CdS followed by a CdTe layer was deposited via vapor deposition, followed by spray coating/thermal treatment of $CdCl_2$. Finally, the CdTe solar cell was completely fabricated by sputtering of a metal layer as back contact. Owing to fabrication of CdTe module, the individual cells were interconnected in series using laser ablation, followed by lamination, in which glass plates were placed and thermally sealed with the glass substrate. At the end of process, the module was encapsulated between two glass plates to form the final module with a less than 10 μm film thickness.

In another work, LCA analysis has been run for CdS/CdTe PV modules in order to estimate primary energy demand, EPBT, and GHG [43]. The results showed EPBT values of 1.7, 1.4 and 1.1 years for the plant scales of 10, 30 and 100 MW/year, which are significantly lower than the EPBTs of a-Si and mc-Si results in the same plant scale. The GHG values of CdS/CdTe PV modules have been ranged as 8.9–14.0 g $CO_{2\text{-eq}}$/kWh for 10–100 MW/year productions. Ito et al. [44] have been illustrated a comparative LCA for a 100-MW PV ground mounting plant, using mc-Si, a-Si, CdTe, and CIS at different module efficiencies. Owing to their results, CIS modules have shorter EPBTs of 1.6 years compared with those of CdTe and a-Si modules, which have 1.9 years and 2.5 years, respectively. The GHG value for these modules has been evaluated in the range of 9–16 g $CO_{2\text{-eq}}$/kWh.

In particular, Fthenakis and Kim [45] conducted LCA studies on thin film technologies, especially CdTe PV modules. With particular discuss about cadmium emissions during the life cycle of modules. Indeed, Zinc smelting/refining is most atmospheric Cd emitting stage with 40 g Cd/ton, They also evaluated the GHG and heavy metal emissions from c-Si, mc-Si, ribbon-Si, and thin film CdTe modules [46] (**Figure 4a**). Environmental emission of cadmium metal from CdTe modules compared with other sources of electricity which illustrate significantly lower heavy metal impact compare to the life cycle of common fossil fuels (see **Figure 4b**). These environmental cadmium emission results show the importance of a general LCA analysis to make a true decision for national renewable energy investment. While CdTe PV systems use Cd element as a main absorber component,

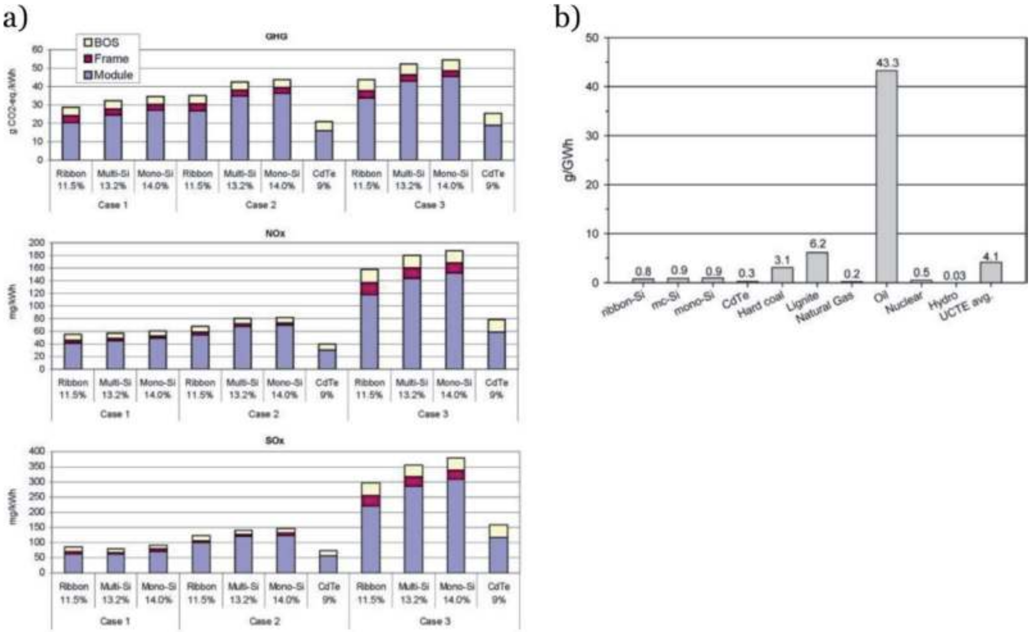

Figure 4.

(a) Life-cycle emissions from silicon and CdTe PV modules. BOS is the balance of system. (b) Life-cycle atmospheric Cd emissions for PV systems from electricity and fuel consumption. The figures are obtained under copyright of American Chemical Society [46].

the emission values show just 0.3 g/GWh which is comparable with the natural gas sources and lower than typical silicon PVs.

In another research, Rocchetti and Beolchini used LCA in order to the management of end-of-life CIGS and CdTe panels [47]. They compared the environmental impacts of the recycling processes for such PV panels, compare with landfill site disposal. Two recycling situation have been evaluated containing conventional and innovative. By using of the conventional method, the modules are crushed and glass components are mechanically recovered. The ethylene-vinyl acetate (EVA) sealing material is passed to thermal treatment for energy generation and the residual material is disposed in a landfill site. On the other hand, the innovative process leads to recover also selenium, indium and gallium from the CIGS panels and tellurium from the CdTe panels as well. However, the potential environmental impacts were similar for the conventional recycling process of both PV panels. Conversely, the innovative recycling of the CdTe panels creates a net production of environmental credits thanks to the recovery of valuable materials. The innovative recycling of CIGS panels has been shown a higher impact compare to the recycling of CdTe panels (2.5 vs. 0.7 kg $CO_{2\text{-eq}}$., respectively, for GHG). In any case, according to LCA results, the disposal of end-of-life panels is not advantageous for the environment. Data obtained with the recycling processes suggest that the innovative recycling is environmentally beneficial only for the CdTe panels, due to the very low content of valuable elements in the CIGS panels. The potential impacts of the management options for the CIGS and CdTe panels in several categories are presented in **Figure 5**. Due to the environmental loads problems, the innovative recycling approach for the CIGS panels was not favorable, in which this refinement option had a high demand of raw materials and energy. In particular, the mentioned recycling management shows a positive correlation with the GHG emission, which generally leads the impact assessment. However, in all categories it is clear that disposal in landfill sites was the worst scenario for the environment.

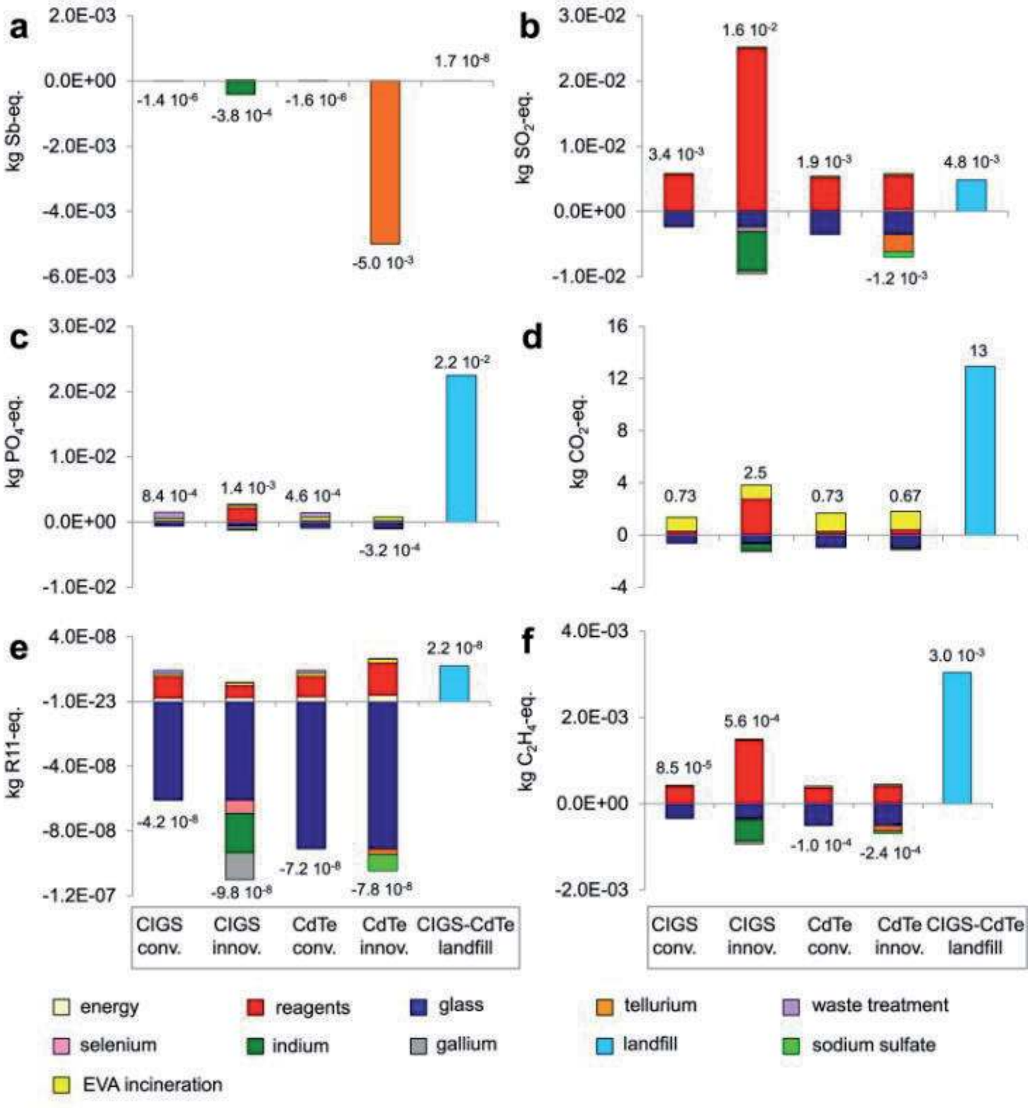

Figure 5.
Potential impacts of the management options for the CIGS and CdTe panels in the categories: (a) abiotic depletion; (b) acidification; (c) eutrophication; (d) global warming; (e) ozone layer depletion (f) photochemical ozone creation. The figure is obtained under copyright of Elsevier [47].

Waste PV panels, depending on the types of PV cells, have different environmental impact potentials due to different contents of substances. Bang et al. [48] have been compared hazardous waste and toxicity potentials, resource depletion from metals in three types of PV modules (CIGS a-Si, mc-Si). Resource depletion and toxicity potentials have been evaluated by using life cycle impact assessment methods and Hazardous waste potentials were examined by using metal leachability tests (**Figure 6**). It is interesting that a-Si PV does not hazardous waste due to Pb/Cadmium or selenium while mc-Si and CIGS PVs have hazardous waste potentials due to lead (Pb) and cadmium/selenium, respectively. Regarding the resource, the mc-Si shows the highest depletion potential due to silver; next highest depletion potential is related to the CIGS due to selenium element; while the lowest rate is for Si PV which is depended to tin and copper. For toxicity potentials, overall the a-Si had lower potentials, derived primarily from Ba/Cu/Ni/Zn elements, than the mc-Si and CIGS PVs of which the toxicity potentials were primarily form Cu/Pb/Ni/Ag and Cu/Hg/Mo/Ni/Ag, respectively. Indeed, waste mc-Si and CIGS PV panels should be recycled and managed with priority.

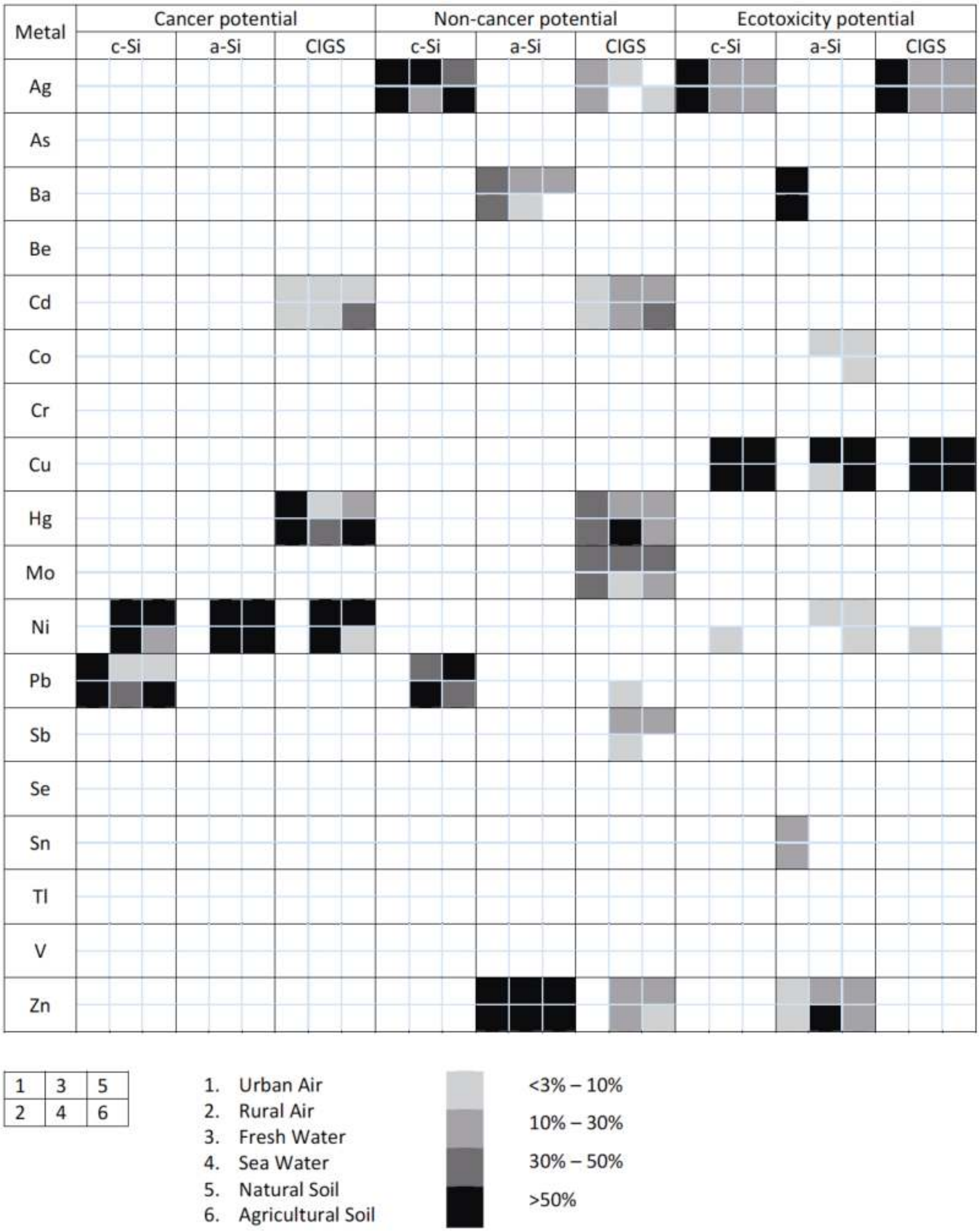

Figure 6.
Toxicity potentials from metals in the PV modules. The share means the proportion of the potential from a given metal to the total from all the metals in each module [48].

2.2 LCA of emerging thin film PVs

Dye-sensitized solar cells (DSCs) are a class of nanomaterial based PVs which show some benefits among other commercial PV systems due to lower production cost and environmental impacts. In the typical DSC fabrication, firstly a transparent conducting oxide (TCO) (e.g., fluorine-doped tin oxide (FTO) and indium-doped tin oxide (ITO)) has been deposited on glass substrates and then it has been covered with a semiconductor material layer, which act as scaffold layer of photoanode. Various nanomaterials and nanocomposite structures have been applied as scaffold photoanode in DSCs [49–55]. After deposition, the coated photoelectrode is sintered in the furnace. Dye sensitizer molecules, such as N719 or organic dyes

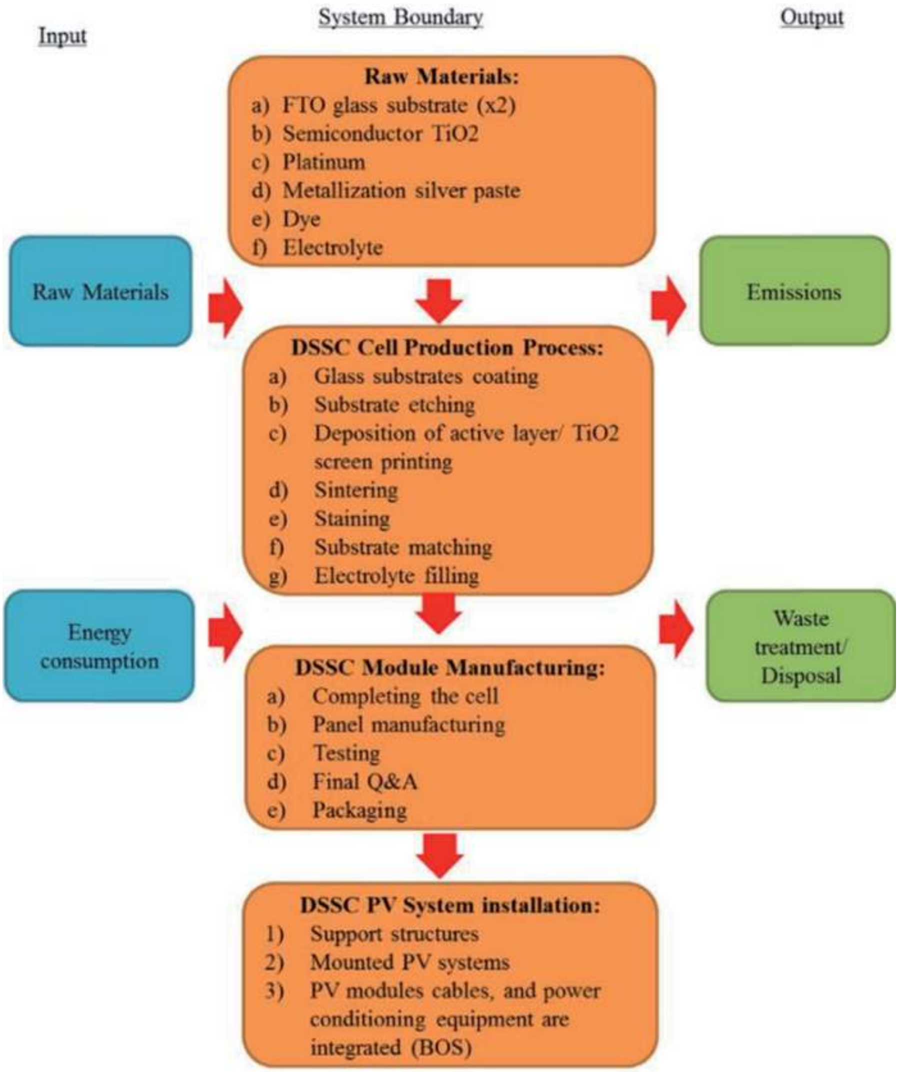

Figure 7.
LCA for DSC process from cradle-to-gate. The figure is obtained under copyright of Elsevier [35].

(such as D35), are then anchored on the photoanode surface to harvest and enhance light absorption [56]. The dye is surrounded by electrolyte solution, containing I^-/I_3^- [57] or Co(II)/Co(III)-complex [58, 59] redox mediators which are dissolved in polar solvents such as acetonitrile or 3-methoxy propionitrile. The counter-electrode is also fabricated by deposition of platinum thin film on FTO or ITO substrates and subsequently the cell is completed by attachment of both electrodes via a thermoplastic polymer. DSC cells are fabricated as large modules. **Figure 7** shows the system boundaries for an example of DSC LCA study.

Few LCA studies have been conducted on DSCs. Greijer et al. [60] evaluated LCA on a DSC system under 2190 kWh/m^2/year solar irradiation. The resulted GHG emissions have been ranged from 19 to 25 g CO$_{2\text{-eq}}$/kWh for DSC module efficiencies ranging between 7 and 12%.

Parisi et al. [61] realized lab-scale environmental analysis on DSC manufacturing. This study assumed efficiency of DSC module as 8% and the module's lifetime assumed 20 years. They demonstrated that the NER, EPBT and CO2 emission values as 12.64, 1.58 years and 22.38 g CO$_{2\text{-eq}}$/kWh, respectively. The authors also compared the LCA results of DSC with some typical thin film PV technologies and showed lower GHG emission and NER values for DSC compared with other organic and inorganic thin films. In another research, Parisi et al. [62] have been reported further LCA on DSCs from previous studies and compared the DSC with other thin film technologies (i.e., polymeric, a-Si, CdTe, and CIS). The environmental impact analysis reported in their work has been performed by using the ReCiPe2008 endpoint level approach associated with a hierarchist perspective. 17 category indicators were Fossil Depletion, Metal Depletion, Agricultural Land Occupation, Natural Land Transformation, Freshwater Ecotoxicity, Freshwater Eutrophication, Urban Land Occupation, Marine Ecotoxicity, Terrestrial Ecotoxicity, Terrestrial Acidification, Climate Change Ecosystems, Ionizing Radiation, Particulate Matter Formation, Photochemical Oxidant Formation, Ozone Depletion, Human Toxicity and Climate Change Human Health. 10 DSC configurations considered in their evaluation (**Table 2**) which in general the DSC with double PET structure show lower environmental impact (**Figure 8**). These results show the effect of PV substrate on environmental life cycle impact, in addition to precursor material.

Based on previous evaluations from many researchers, the range CED, EPBT and GHG emissions rate of DSCs are 277–365 MJ/m^2, 0.6–1.8 years and 9.8–120.0 g $CO_{2\text{-eq}}$/kWh, respectively. It is notably that also the GHG emissions of DSC strongly related to the operational lifetime of DSC modules. The best performance of DSC could be obtained with higher conversion efficiencies and longer lifetimes.

Recently, single-junction polymer solar cells (OPVs) can attract the PV community attention due to possibility of roll-to-roll printing fabrication. Lizin et al. [63] focused on the environmental impact of OPVs. They used a P3HT/$PC_{60}BM$ active layer blend processed on semi-industrial pilot lines which is working under ambient conditions. Both standard and inverted device structures have been used in their work. The general steps in the LCA framework were standardized according to the ISO 14000 series which is shown in **Figure 9**.

The environmental impact was found to be strongly decreased through continuous manufacturing procedures. The current top performing cell regarding environmental performance has an energy payback time in the order of months and a cumulative energy demand of 37.58 MJp m^2 for cells having 2% efficiency.

In the past few years, Quantum dot sensitized solar cell (QDSC) was introduced based on the DSC structure as an alternative dye because of its high absorption coefficient, photostability and low cost [64]. Various QD materials such as CdS, CdTe, CdSe, ZnSe, PbS and InAs have been used as sensitizer to absorb visible light of solar irradiation. The typical structure of QDSC is similar to DSC, which

Configuration	Abbreviation
Glass–liquid electrolyte–platinum–glass	A
Glass–ionic liquid (type 3)–platinum–glass	B
Glass–ionic liquid (type 6)–platinum–glass	C
Glass–ionic liquid(type7)–platinum–glass	D
Steel–liquid electrolyte–platinum–glass	E
Steel–liquid electrolyte–platinum–PET	F
PET–liquid electrolyte–platinum–glass	G
PET–liquid electrolyte–platinum–PET	H
Glass–ionic liquid(type1)–cobalt sulfide–PET	I
Glass–liquid electrolyte–carbon	L

Table 2.
DSC configuration of LCA analysis obtained from ref [62].

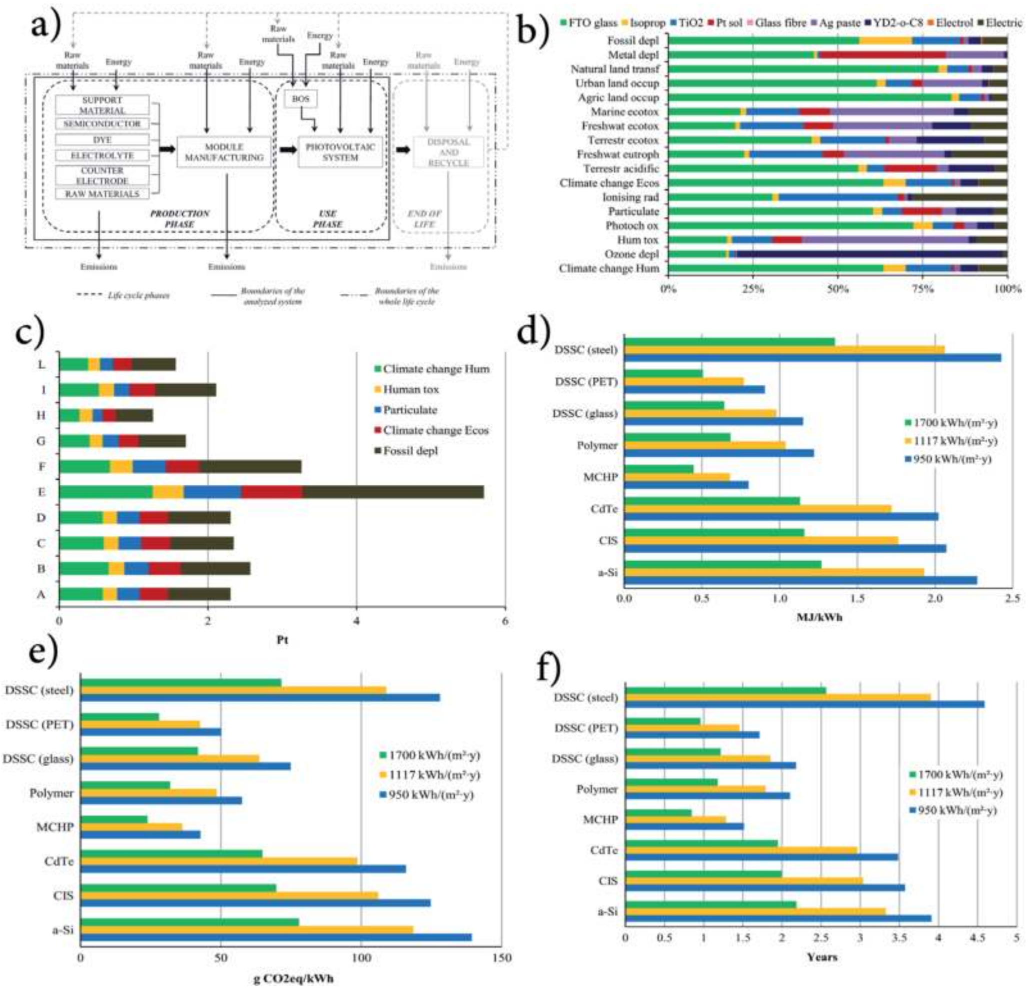

Figure 8.
(a) Designed boundaries of LCA evaluation of DSCs. (b) LCA characterization diagram of DSC module (containing YD2-o-C8 dye and CoII/CoIII redox couple). (c) Diagram of ReCiPe2008 single score analysis for DSC modules configurations. The calculated CED (d), GWP (e) and EPBT (f) indicators for kWh electricity production of different PV modules. The figures are obtained under copyright of Elsevier [62].

consists of counter and photoanode electrodes, but the only difference is that dye is replaced with QD materials in this structure [65]. Different techniques have been utilized to produce QD sensitizers coated on mesoporous TiO_2 either by in-situ or ex-situ fabrication [66]. There are two well known in-situ fabrication methods, (1) Chemical Bath Deposition (CBD) and (2) Successive Ionic Layer Adsorption and Reaction (SILAR). These methods have been generally used due to applicability in large-scale production [66]. Roll to-roll coating process has been also introduced for fabrication of large scale QDSC, before module encapsulation and framing.

Sengül and Theis evaluated LCA on a proposed type of nanostructure, QDPV module [67] using a roll-to-roll manufacturing process (**Figure 10**). The LCA parameters evaluated and compared with other PV and energy resources. Furthermore, emission of NO_x and SO_x gases and several heavy metals such as, mercury, nickel, arsenic, chromium, cadmium, and lead are evaluated for QDPVs and compared with other PV technologies. Their results indicate that while QDPV modules have shorter EPBT, lower Global Warming Potential (GWP), SO_x and NOx emissions than other types of PV modules, they have higher heavy metal emissions.

As a flagship of emerging thin film technologies, Perovskite Solar Cells (PSCs) obtain a remarkable increase of the power conversion efficiency (PCE) leading

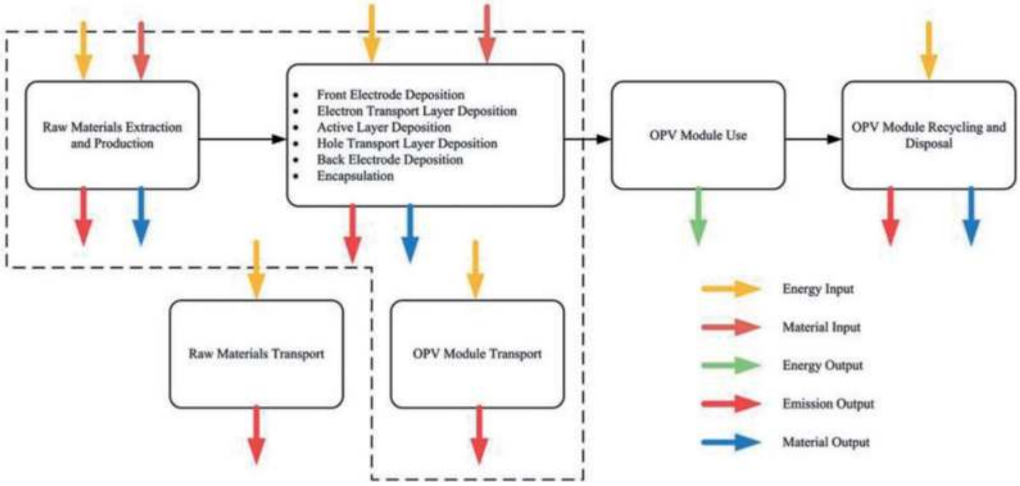

Figure 9.
OPV life cycle analysis scope definition the figure is obtained under copyright of Royal Society of Chemistry [63].

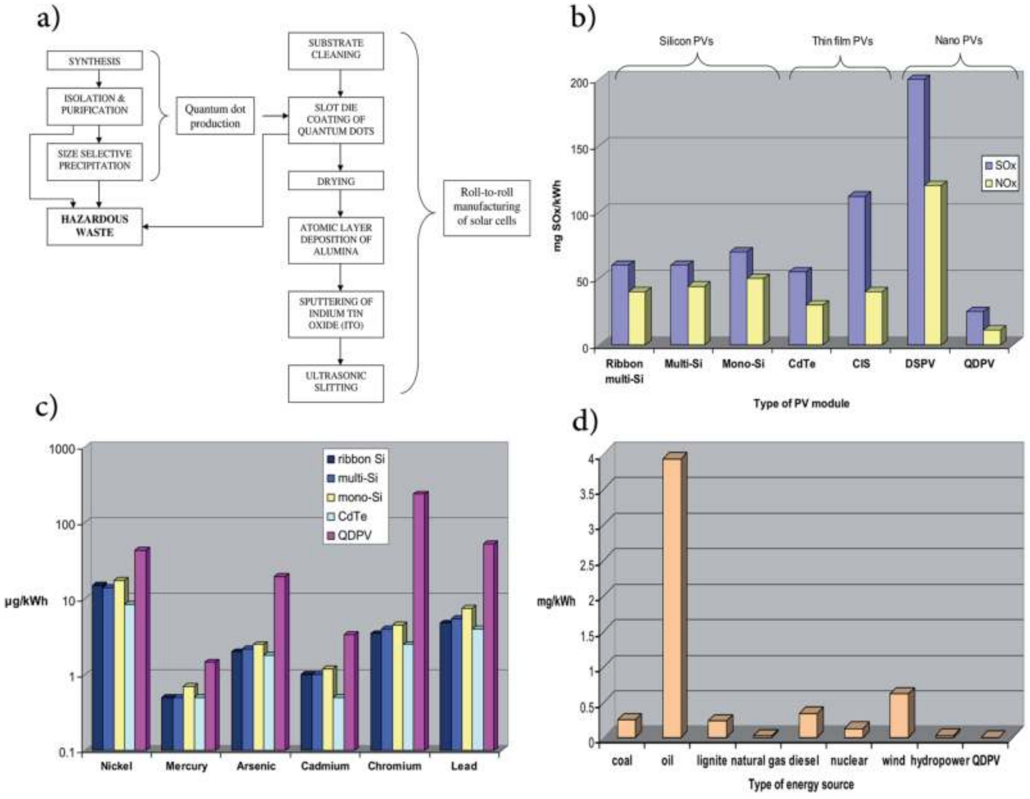

Figure 10.
(a) A typical quantum dot solar cell production process. (b) Comparison of emissions of sulfur oxides and nitrogen oxides for QDPV modules with different types of PV modules. (c) Comparison of heavy metal emissions from QDPV modules with silicon and CdTe PV modules. (d) Total amount of heavy metal emissions from QDPV modules compared to heavy metal emissions from other types of energy sources. The figures are obtained under copyright of Elsevier [67].

to a certified efficiency of 24.2% [4]. The excellence of PSCs marks a revolution among PVs by promising combination of low cost procedure (solution based) and high efficiency while in the typical commercial PV modules, manufacturing of the semiconductor absorber layer is an energy intensive process. High recorded values of the power conversion efficiency (PCE) is related to outstanding characteristics of hybrid perovskite such as, long carrier lifetimes, broad absorption and strong diffusion lengths, defect tolerance, direct band-gap and low recombination. These outstanding properties of hybrid perovskite led to various applications [68–71]. PSCs usually consist of a conductive substrate (FTO or ITO), an electron selective layer (ESL), a perovskite absorber, a hole transporting material (HTM) and a back contact electrode (gold, silver or carbon). Many inorganic structures have been utilized as ESL such as metal oxides, including TiO_2 (mesoscopic and planar structures) [18], ZnO [72] and SnO_2 [73], as well as polyoxometalates [74] which can provide low-temperature fabrication in addition to high efficiencies. Deposition of the hybrid perovskite is one of the main challenges for a high-reproducible, atmosphere-independent PSC fabrication technique due to air-sensitive nature of perovskite layer. In particular, Yaghoobi Nia et al. have developed a Crystal Engineering (CE) approach for kinetically controlling the perovskite phase nucleation and subsequently crystal growth under ambient conditions, through the formation of a lead based intermediate phase, reaching high efficiency $MAPbI_3$-based PSCs (more than 17%) and perovskite solar modules (~13%) [18] (**Figure 11**) which represent a promising approach for future up-scaling and commercial programs of PSCs.

The system boundary of a cradle-to-grave LCA study for a typical PSC system is presented in **Figure 12a** [75].

Raw materials extraction is classified at first stage while preparation of the precursors, such as FTO glass, TiO_2, PbI_2, Au, and PET materials, to be defined in the second stage. Fabrication of the mentioned perovskite module consists of, (1) laser ablation of the FTO glass substrates to define the cell arrays, (2) deposition of blocking TiO2 layer, (3) electron transport layer deposition (ETL), (4) perovskite layer deposition on the ETL (n-i-p structure), (5) hole transport layer (HTL) deposition, and finally (6) deposition of gold by thermal evaporation as back contact electrode [75]. The modules have been encapsulated by PET polymers. After assembling of the modules, they have been utilized to generate electricity from sun light. At the end, the waste modules have been landfilled in the disposal stage without any recycling program.

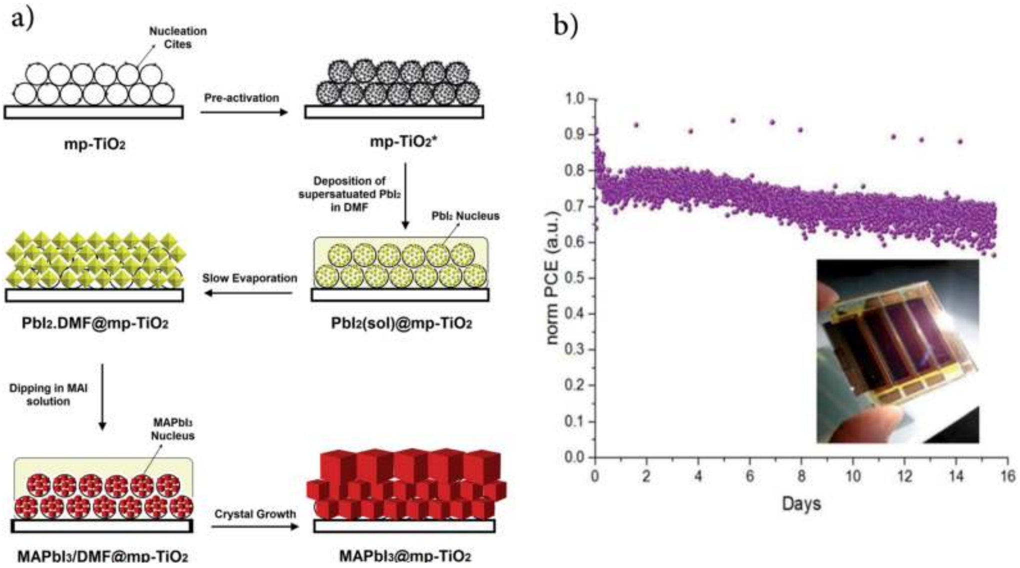

Figure 11.
(a) A schematic presentation of crystal engineering (CE) approach in order to fabrication perovskite solar modules under ambient condition. (b) Light-soaking stability test results of the presented PSC which is fabricated through CE. The figures are obtained under copyright of Royal Society of Chemistry [18].

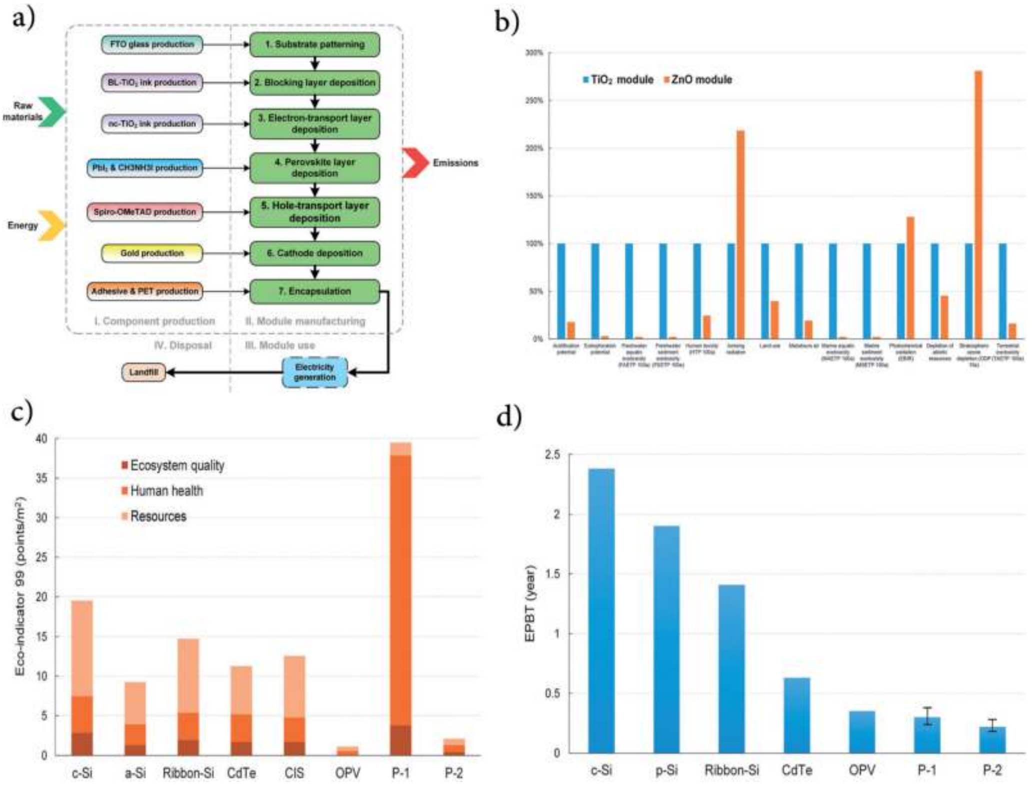

Figure 12.
(a) System boundary of manufacturing a perovskite solar module using TiO_2 as ETL. (b) Life cycle impact assessment comparison between 1 m^2 of the TiO_2 module and 1 m^2 of the ZnO module. (c) Eco-indicator 99 results for 1 m^2 of eight PV modules. P-1 represents the TiO_2 perovskite module; P-2 represents the ZnO perovskite module. (d) Energy payback time for seven PV modules. P-1 represents the TiO_2 perovskite module; P-2 represents the ZnO perovskite module. The figures are obtained under copyright of Royal Society of Chemistry [75].

Celik et al. [76] have been assessed cradle-to-gate the environmental impacts for three PSC modules consist of, vacuum, solution, and HTM-free structures, considering of 15% module efficiency, 15-year life span, and 65% active area under 1700 $kWh/m^2/year$ solar irradiation. Owing to their results, EPBT and GHG emissions of the perovskite modules could be ranged between 1.05 and 1.54 years and 100 to 150 g $CO_{2\text{-}eq}/kWh$, respectively, which can be considered as lower values when compare with crystalline and commercial thin film technologies.

In particular, Gong et al. [75] have been evaluated LCA of two types of perovskite solar modules with two different ETLs (ZnO and TiO_2) by cradle to-grave approach to observe 16 LCIs and two sustainable indicators, namely, EPBT and GHG emission, under irradiation of 1960 $kWh/m^2/year$, assuming a lifetime of 2 years and PR of 0.80. The authors found that primary energy which is consumed by TiO_2 and ZnO modules are 446 MJ/m^2 and 392 MJ/m^2, respectively while GHG emission values calculated as 2.17 and 1.91 g $CO_{2\text{-}eq}/m^2$ respectively for TiO2 and ZnO modules.

The comparison of life cycle impact assessment results between the two modules is presented in (**Figure 12b**). It is evidenced that the ZnO module performs in a more environmental friendly manner except three impact categories: (1) photochemical oxidation, (2) ionizing radiation, and (3) stratospheric ozone depletion. Furthermore, in **Figure 12c** there is a comparison of Eco-indicator 99 results for eight types of PV modules. ZnO module has been achieved the second lowest level for three damage categories (ecosystem quality, resources and human health).

The Eco-indicator 99 values of the ZnO module are one order of magnitude lower than the values for c-Si, a-Si, ribbon-Si, CdTe, CIS, and the TiO_2 module. The EPBT comparison among seven PV modules is shown in **Figure 12d**. The ZnO perovskite module has been shown the lowest EPBT value of 0.22 years. The OPV module just shows a slightly longer EPBT values. The outstanding performance against silicon-based and CdTe modules is higher potential for a roll-to-roll process [77]. The EPBT of a perovskite module can be rapidly reduced in the near future by using more efficient processing technologies [18]. In particular, the LCA results of perovskite solar modules show the importance of the ETL layer in the case of material and deposition process which need to carefully considered in the scale-up research activities.

Summing up, the reports of LCA for perovskite solar cells show the EPBT varied from 0.2 to 5.4 years and the GHG emissions rate within 56.65–497.2 g $CO_{2\text{-eq}}$/kWh. Compared with silicon and thin film technologies, perovskite solar cells perform much lower energy consumption with competitive environmental benefits and EPBT which pave the way toward industrial manufacturing.

One of the important environmental concerns for perovskite solar cells is related to using of lead as an important element of active layer. Recently in an interesting activity, Yoo et al. [78] have been used Environmental Fate Modeling (EFM) model in order to evaluate of the lead compounds exposure in PSCs and their impact on the environment and humans ecosystem. Two main accidental situations of such compounds, have been considered as fire (formation of PbO) and flooding (formation of PbI_2). The results show water systems as the most unprotected to the toxicity of lead exposure. Accordingly, the assessments have been conducted into two categories, (1) upper limit suggestion for PSC production per unit area through the Predicted Environmental Concentrations (PEC) of PbI_2 and PbO, (2) lower limit suggestion of the demand safety management area through PEC evaluation in various environmental areas., PEC_{soil} values show ~10^3 less than the Predicted No Effect Concentration (PNEC) values for both compounds even using more than 100 MW power plant. The PEC_{soil} of PbI_2 is calculated as 1.4 ppm from 100 MW of PSC plants, while that of PbO is 3 ppm. An industrial power generation scale of 10 GW should exist in a 1 km^2 area to reach the concentrations near the PNEC values. Thus, the environmental risks on the soil concentrations could be classified as insignificant. However, the mentioned lead compounds can also penetrate into water resources. The risk factor of PbI_2 and PbO could be reached 1 when the PV plant scale reaches 21.8 and 6.39 MW km^{-2}, respectively. Therefore, the partitioning strategies of lead compounds per unit of PSC output generation plant, near water sources should be carefully considered for define the regulations by limiting the plant scale per unit area.

3. Conclusions

This chapter reviewed several previous environmental impact assessment studies on commercial and emerging thin film solar PV technologies including a-Si, CdTe, CIGS, DSC, PSC, OPV and QDSC. Three main indicators of LCA, such as CED, EPBT, and GWP, are considered and summarized. Across the analysis, emerging thin film PVs, especially perovskite solar cells, demonstrated the lowest energy requirement and shorter EPBT among other conventional PV technologies due to its high efficiency, low-cost production and eco-compatibility. Furthermore, the general life cycle assessment results show that the concern related to environmental impacts of heavy metal emission of some thin film PV technologies, particularly CdTe (emission of Cd) and PSCs (emission of Pb), is not noticeable when compare with life cycle of wafer based commercial PVs and typical fossil fuels. However, the environmental fate modeling results show that the effect of various environmental and human factors should be assessed and safety standards should be established using the most conservative range among various environmental evaluation results. Lastly, we conclude that, low-temperature solution-based produced perovskite solar modules are potentially the most environmentally sustainable PV if future development confirms a larger performance ratio and a longer lifetime.

Acknowledgements

Authors gratefully acknowledge the supports from Kimia Solar Co. and IRITALY Trading Company S.r.l.

Conflict of interest

The authors declare no conflict of interest.

Author details

Mahmoud Zendehdel[1]*, Narges Yaghoobi Nia[2] and Mohammadreza Yaghoubinia[1,3]

1 K.S.R.I (Kimia Solar Research Institute), Kimia Solar Company, Kashan, Iran

2 CHOSE (Centre for Hybrid and Organic Solar Energy), University of Rome "Tor Vergata", Rome, Italy

3 Mobarakeh Steel Company, Mobarakeh, Esfahan, Iran

*Address all correspondence to: m.zendehdel@kimiasolar.com

References

[1] Demirbas MF. Electricity production using solar energy. Energy Sources Part A-recovery Utilization and Environmental Effects. 2007;**29**(6):563-569. DOI: 10.1080/009083190957685

[2] Jean J, Brown PR, Jaffe RL, Buonassisi T, Bulović V. Pathways for solar photovoltaics. Energy & Environmental Science. 2015;**8**(4): 1200-1219. Available from: http://xlink.rsc.org/?DOI=C4EE04073B

[3] Czochralski J. Ein neues verfahren zur messung der kristallisationsgeschwindigkeit der metalle scholar. Zeitschrift für Physikalische Chemie. 2017;**92U**(1):219-221. Available from: https://www.degruyter.com/view/j/zpch.1918.92.issue-1/zpch-1918-9212/zpch-1918-9212.xml

[4] National Renewable Energy Laboratory. Best Research-Cell Efficiency Chart|Photovoltaic Research|NREL [Internet]. Available from: https://www.nrel.gov/pv/cell-efficiency.html [Accessed: 04-March-2019]

[5] Yablonovitch E, Gmitter T, Harbison JP, Bhat R. Extreme selectivity in the lift-off of epitaxial GaAs films. Applied Physics Letters. 1987;**51**(26):2222-2224. DOI: 10.1063/1.98946

[6] Shah AV, Schade H, Vanecek M, Meier J, Vallat-Sauvain E, Wyrsch N, et al. Thin-film silicon solar cell technology. Progress in Photovoltaics: Research and Applications. 2004;**12**(23):113-142. DOI: 10.1002/pip.533

[7] Staebler DL, Wronski CR. Reversible conductivity changes in discharge-produced amorphous Si. Applied Physics Letters. 1977;**31**(4):292-294. DOI: 10.1063/1.89674

[8] Kessler F, Rudmann D. Technological aspects of flexible CIGS solar cells and modules. Solar Energy. 2004;**77**(6):685-695. Available from: https://www.sciencedirect.com/science/article/pii/S0038092X04000854

[9] Hetzer MJ, Strzhemechny YM, Gao M, Contreras MA, Zunger A, Brillson LJ. Direct observation of copper depletion and potential changes at copper indium gallium diselenide grain boundaries. Applied Physics Letters. 2005;**86**(16):162105. DOI: 10.1063/1.1906331

[10] Werner JH, Mattheis J, Rau U. Efficiency limitations of polycrystalline thin film solar cells: Case of Cu(In,Ga)Se2. Thin Solid Films. 2005;**480-481**:399-409. Available from: https://www.sciencedirect.com/science/article/pii/S0040609004016128

[11] Nishiwaki S, Siebentritt S, Walk P, Lux-Steiner MC. A stacked chalcopyrite thin-film tandem solar cell with 1.2 V open-circuit voltage. Progress in Photovoltaics: Research and Applications. 2003;**11**(4):243-248. DOI: 10.1002/pip.486

[12] Todorov TK, Tang J, Bag S, Gunawan O, Gokmen T, Zhu Y, et al. Beyond 11% efficiency: Characteristics of state-of-the-art $Cu_2ZnSn(S,Se)_4$ solar cells. Advanced Energy Materials. 2013;**3**(1):34-38. DOI: 10.1002/aenm.201200348

[13] Mendis BG, Shannon MD, Goodman MC, Major JD, Claridge R, Halliday DP, et al. Direct observation of Cu, Zn cation disorder in Cu_2ZnSnS_4 solar cell absorber material using aberration corrected scanning transmission electron microscopy. Progress in Photovoltaics: Research and Applications. 2014;**22**(1):24-34. DOI: 10.1002/pip.2279

[14] Kim H-S, Lee C-R, Im J-H, Lee K-B, Moehl T, Marchioro A, et al. Lead iodide Perovskite sensitized all-solid-state submicron thin film Mesoscopic solar cell with efficiency exceeding 9%. Scientific Reports. 2012;**2**(1):591. Available from: http://www.nature.com/articles/srep00591

[15] Eperon GE, Stranks SD, Menelaou C, Johnston MB, Herz LM, Snaith HJ. Formamidinium lead trihalide: A broadly tunable perovskite for efficient planar heterojunction solar cells. Energy & Environmental Science. 2014;**7**(3):982. Available from: http://xlink.rsc.org/?DOI=c3ee43822h

[16] Hao F, Stoumpos CC, Cao DH, Chang RPH, Kanatzidis MG. Lead-free solid-state organic–inorganic halide perovskite solar cells. Nature Photonics. 2014;**8**(6):489-494

[17] Noh JH, Im SH, Heo JH, Mandal TN, Seok S II. Chemical Management for Colorful, efficient, and stable inorganic–organic hybrid nanostructured solar cells. Nano Letters. 2013;**13**(4):1764-1769. DOI: 10.1021/nl400349b

[18] Yaghoobi Nia N, Zendehdel M, Cinà L, Matteocci F, Di Carlo A. A crystal engineering approach for scalable perovskite solar cells and module fabrication: A full out of glove box procedure. Journal of Materials Chemistry A. 2018;**6**(2):659-671. Available from: http://xlink.rsc.org/?DOI=C7TA08038G

[19] Liu M, Johnston MB, Snaith HJ. Efficient planar heterojunction perovskite solar cells by vapour deposition. Nature. 2013;**501**(7467):395-398. Available from: http://www.ncbi.nlm.nih.gov/pubmed/24025775

[20] Xing G, Mathews N, Sun S, Lim SS, Lam YM, Gratzel M, et al. Long-range balanced electron- and hole-transport lengths in organic-inorganic CH3NH3PbI3. Science. 2013;**342**(6156):344-347

[21] Ball JM, Lee MM, Hey A, Snaith HJ. Low-temperature processed meso-superstructured to thin-film perovskite solar cells. Energy & Environmental Science. 2013;**6**(6):1739. Available from: http://xlink.rsc.org/?DOI=c3ee40810h

[22] Peumans P, Yakimov A, Forrest SR. Small molecular weight organic thin-film photodetectors and solar cells. Journal of Applied Physics. 2003;**93**(7):3693-3723. DOI: 10.1063/1.1534621

[23] Li G, Zhu R, Yang Y. Polymer solar cells. Nature Photonics. 2012;**6**(3):153-161. Available from: http://www.nature.com/articles/nphoton.2012.11

[24] Krebs FC, Gevorgyan SA, Alstrup J. A roll-to-roll process to flexible polymer solar cells: Model studies, manufacture and operational stability studies. Journal of Materials Chemistry. 2009;**19**(30):5442. Available from: http://xlink.rsc.org/?DOI=b823001c

[25] Kim JY, Lee K, Coates NE, Moses D, Nguyen T-Q, Dante M, et al. Efficient tandem polymer solar cells fabricated by all-solution processing. Science. 2007;**317**(5835):222-225

[26] Günes S, Neugebauer H and, Sariciftci NS. Conjugated polymer-based organic solar cells. Chemical Reviews. 2007;**107**(4):1324-1338. DOI: 10.1021/cr050149z

[27] Kawano K, Pacios R, Poplavskyy D, Nelson J, Bradley DDC, Durrant JR. Degradation of organic solar cells due to air exposure. Solar Energy Materials & Solar Cells. 2006;**90**(20):3520-3530. Available from: https://www.sciencedirect.com/science/article/pii/S0927024806002960

[28] Lunt RR, Osedach TP, Brown PR, Rowehl JA, Bulović V. Practical roadmap

and limits to nanostructured photovoltaics. Advanced Materials. 2011;**23**(48):5712-5727. DOI: 10.1002/adma.201103404

[29] Hagfeldt A, Boschloo G, Sun L, Kloo L, Pettersson H. Dye-sensitized solar cells. Chemical Reviews. 2010;**110**(11):6595-6663. DOI: 10.1021/cr900356p

[30] Yella A, Lee H-W, Tsao HN, Yi C, Chandiran AK, Nazeeruddin MK, et al. Porphyrin-sensitized solar cells with cobalt (II/III)-based redox electrolyte exceed 12 percent efficiency. Science. 2011;**334**(6056):629-634. Available from: http://www.ncbi.nlm.nih.gov/pubmed/22053043

[31] Lan X, Masala S, Sargent EH. Charge-extraction strategies for colloidal quantum dot photovoltaics. Nature Materials. 2014;**13**(3):233-240. Available from: http://www.nature.com/articles/nmat3816

[32] Wang X, Koleilat GI, Tang J, Liu H, Kramer IJ, Debnath R, et al. Tandem colloidal quantum dot solar cells employing a graded recombination layer. Nature Photonics. 2011;**5**(8):480-484. Available from: http://www.nature.com/articles/nphoton.2011.123

[33] Chuang C-HM, Brown PR, Bulović V, Bawendi MG. Improved performance and stability in quantum dot solar cells through band alignment engineering. Nature Materials. 2014;**13**(8):796-801. Available from: http://www.nature.com/articles/nmat3984

[34] Zhitomirsky D, Voznyy O, Levina L, Hoogland S, Kemp KW, Ip AH, et al. Engineering colloidal quantum dot solids within and beyond the mobility-invariant regime. Nature Communications. 2014;**5**(1):3803. Available from: http://www.nature.com/articles/ncomms4803

[35] Ludin NA, Mustafa NI, Hanafiah MM, Ibrahim MA, Asri Mat Teridi M, Sepeai S, et al. Prospects of life cycle assessment of renewable energy from solar photovoltaic technologies: A review. Renewable and Sustainable Energy Reviews. 2018;**96**:11-28. Available from: https://www.sciencedirect.com/science/article/pii/S1364032118305574

[36] Godlee F. An international standard for disclosure of clinical trial information. BMJ. 2006;**332**(7550):1107-1108. Available from: http://www.ncbi.nlm.nih.gov/pubmed/16690647

[37] Yi S, Kurisu KH, Hanaki K. Life cycle impact assessment and interpretation of municipal solid waste management scenarios based on the midpoint and endpoint approaches. International Journal of Life Cycle Assessment. 2011;**16**(7):652-668. DOI: 10.1007/s11367-011-0297-3

[38] Rolf F, Garvin H, Marco R, Parikhit S, de Wild-Scholten M. Methodology Guidelines on Life Cycle Assessment of Photovoltaic Electricity. 3rd ed. Golden, CO (United States): National Renewable Energy Lab. (NREL); 2016. Available from: https://www.osti.gov/biblio/1351599

[39] Peng J, Lu L, Yang H. Review on life cycle assessment of energy payback and greenhouse gas emission of solar photovoltaic systems. Renewable and Sustainable Energy Reviews. 2013;**19**:255-274. Available from: https://www.sciencedirect.com/science/article/pii/S1364032112006478

[40] Pacca S, Sivaraman D, Keoleian GA. Parameters affecting the life cycle performance of PV technologies and systems. Energy Policy. 2007;**35**(6):3316-3326. Available from: https://www.sciencedirect.com/science/article/pii/S0301421506003715?via%3Dihub

[41] Minemoto T, Nagae S, Takakura H. Impact of spectral irradiance distribution and temperature on the outdoor performance of amorphous Si photovoltaic modules. Solar Energy Materials & Solar Cells. 2007;**91**(10):919-923. Available from: https://www.sciencedirect.com/science/article/pii/S0927024807000712

[42] Fthenakis VM. Life cycle impact analysis of cadmium in CdTe PV production. Renewable and Sustainable Energy Reviews. 2004;**8**(4):303-334. Available from: https://www.sciencedirect.com/science/article/pii/S1364032103001345?via%3Dihub

[43] Kato K, Hibino T, Komoto K, Ihara S, Yamamoto S, Fujihara H. A life-cycle analysis on thin-film CdS/CdTe PV modules. Solar Energy Materials & Solar Cells. 2001;**67**(1-4):279-287. Available from: https://www.sciencedirect.com/science/article/pii/S0927024800002932?via%3Dihub

[44] Ito M, Kato K, Komoto K, Kichimi T, Kurokawa K. A comparative study on cost and life-cycle analysis for 100 MW very large-scale PV (VLS-PV) systems in deserts using m-Si, a-Si, CdTe, and CIS modules. Progress in Photovoltaics: Research and Applications. 2008;**16**(1):17-30. DOI: 10.1002/pip.770

[45] Fthenakis VM, Kim HC. CdTe photovoltaics: Life cycle environmental profile and comparisons. Thin Solid Films. 2007;**515**(15):5961-5963. Available from: https://www.sciencedirect.com/science/article/pii/S0040609006016361?via%3Dihub

[46] Fthenakis VM, Kim HC, Alsema E. Emissions from photovoltaic life cycles. Environmental Science & Technology. 2008;**42**(6):2168-2174. DOI: 10.1021/es071763q

[47] Rocchetti L, Beolchini F. Recovery of valuable materials from end-of-life thin-film photovoltaic panels: Environmental impact assessment of different management options. Journal of Cleaner Production. 2015;**89**:59-64. Available from: https://www.sciencedirect.com/science/article/pii/S0959652614011809?via%3Dihub

[48] Bang Y-Y, Hong N-J, Sung Lee D, Lim S-R. Comparative assessment of solar photovoltaic panels based on metal-derived hazardous waste, resource depletion, and toxicity potentials. International Journal of Green Energy. 2018;**15**(10):550-557. DOI: 10.1080/15435075.2018.1505618

[49] Habibi MH, Karimi B, Zendehdel M, Habibi M. Fabrication, characterization of two nano-composite CuO-ZnO working electrodes for dye-sensitized solar cell. Spectrochimica Acta Part A. 2013;**116**:374-380

[50] Habibi MH, Habibi AH, Zendehdel M, Habibi M. Dye-sensitized solar cell characteristics of nanocomposite zinc ferrite working electrode: Effect of composite precursors and titania as a blocking layer on photovoltaic performance. Spectrochimica Acta Part A. 2013;**110**:226-232

[51] Hossein Habibi M, Askari E, Habibi M, Zendehdel M. Novel nanostructure zinc zirconate, zinc oxide or zirconium oxide pastes coated on fluorine doped tin oxide thin film as photoelectrochemical working electrodes for dye-sensitized solar cell. Spectrochimica Acta Part A. 2013;**104**:197-202

[52] Habibi MH, Mikhak M, Zendehdel M, Habibi M. Influence of nanostructured zinc titanate, zinc oxide or titanium dioxide thin film coated on fluorine doped tin oxide as working electrodes for dye-sensitized solar cell. International Journal of Electrochemical Science. 2012;**7**(8):6787

[53] Habibi MH, Karimi B, Zendehdel M, Habibi M. Preparation of nanostructure mixed copper-zinc oxide via co-precipitation rout for dye-sensitized solar cells: The influence of blocking layer and Co(II)/Co(III) complex redox shuttle. Journal of Industrial and Engineering Chemistry. 2014;**20**(4):1462-1467. Available from: https://www.sciencedirect.com/science/article/pii/S1226086X13003432

[54] Habibi MH, Mardani M, Habibi M, Zendehdel M. Enhanced photovoltage (Voc) of nano-structured zinc tin oxide (ZTO) working electrode prepared by a green hydrothermal route for dye-sensitized solar cell (DSSC). Journal of Materials Science: Materials in Electronics. 2017;**28**(4):3789-3795. DOI: 10.1007/s10854-016-5989-9

[55] Karimian D, Yadollahi B, Zendehdel M, Mirkhani V. Efficient dye-sensitized solar cell with a pure thin film of a hybrid polyoxometalate covalently attached organic dye as a working electrode in a cobalt redox mediator system. RSC Advances. 2015;**5**(94):76875-76882. Available from: http://xlink.rsc.org/?DOI=C5RA09104G

[56] Gong J, Liang J, Sumathy K. Review on dye-sensitized solar cells (DSSCs): Fundamental concepts and novel materials. Renewable and Sustainable Energy Reviews. 2012;**16**(8):5848-5860. Available from: https://www.sciencedirect.com/science/article/pii/S136403211200319X?via%3Dihub

[57] Su'ait MS, Rahman MYA, Ahmad A. Review on polymer electrolyte in dye-sensitized solar cells (DSSCs). Solar Energy. 2015;**115**:452-470. Available from: https://www.sciencedirect.com/science/article/pii/S0038092X15001139?via%3Dihub

[58] Yaghoobi Nia N, Farahani P, Sabzyan H, Zendehdel M, Oftadeh M. A combined computational and experimental study of the $[Co(bpy)_3]^{2+/3+}$ complexes as one-electron outer-sphere redox couples in dye-sensitized solar cell electrolyte media. Physical Chemistry Chemical Physics. 2014;**16**(23):11481-11491

[59] Nasr-Esfahani M, Zendehdel M, Yaghoobi Nia N, Jafari B, Khosravi BM. Fabrication and characterization of a new dye sensitized solar cell with a new Schiff base cobalt complex as a redox mediator. RSC Advances. 2014;**4**(31):1596

[60] Greijer H, Karlson L, Lindquist S-E, Hagfeldt A. Environmental aspects of electricity generation from a nanocrystalline dye sensitized solar cell system. Renewable Energy. 2001;**23**(1):27-39. Available from: https://www.sciencedirect.com/science/article/pii/S0960148100001117?via%3Dihub

[61] Parisi M, Sinicropi A, Basosi R. Life cycle assessment of gratzel-type cell production for non conventional photovoltaics from novel organic dyes. International Journal of Heat and Technology. 2011;**29**:161-169

[62] Parisi ML, Maranghi S, Basosi R. The evolution of the dye sensitized solar cells from Grätzel prototype to up-scaled solar applications: A life cycle assessment approach. Renewable and Sustainable Energy Reviews. 2014;**39**:124-138. Available from: https://www.sciencedirect.com/science/article/pii/S1364032114005310?via%3Dihub

[63] Lizin S, Van Passel S, De Schepper E, Maes W, Lutsen L, Manca J, et al. Life cycle analyses of organic photovoltaics: A review. Energy & Environmental Science. 2013;**6**(11):3136. Available from: http://xlink.rsc.org/?DOI=c3ee42653j

[64] Shen Y-J, Lee Y-L. Assembly of CdS quantum dots onto mesoscopic TiO_2 films for quantum dot-sensitized solar cell applications. Nanotechnology.

2008;**19**(4):045602. Available from: http://stacks.iop.org/0957-4484/19/i=4/a=045602?key=crossref.19ab08e1206f98636af4427396a516fd

[65] Sudhagar P, Jung JH, Park S, Sathyamoorthy R, Ahn H, Kang YS. Self-assembled CdS quantum dots-sensitized TiO2 nanospheroidal solar cells: Structural and charge transport analysis. Electrochimica Acta. 2009;**55**(1):113-117. Available from: https://www.sciencedirect.com/science/article/pii/S0013468609010561?via%3Dihub

[66] Jun HK, Careem MA, Arof AK. Quantum dot-sensitized solar cells—Perspective and recent developments: A review of Cd chalcogenide quantum dots as sensitizers. Renewable and Sustainable Energy Reviews. 2013;**22**:148-167. Available from: https://www.sciencedirect.com/science/article/pii/S1364032113000610?via%3Dihub

[67] Şengül H, Theis TL. An environmental impact assessment of quantum dot photovoltaics (QDPV) from raw material acquisition through use. Journal of Cleaner Production. 2011;**19**(1):21-31. Available from: https://www.sciencedirect.com/science/article/pii/S0959652610003252

[68] Salamandra L, Yaghoobi Nia N, Di Natali M, Fazolo C, Maiello S, La Notte L, et al. Perovskite photo-detectors (PVSK-PDs) for visible light communication. Organic Electronics. 2019;**69**:220-226. Available from: https://www.sciencedirect.com/science/article/pii/S1566119919301090?dgcid=rss_sd_all

[69] Taheri B, Yaghoobi Nia N, Agresti A, Pescetelli S, Ciceroni C, Del Rio Castillo AE, et al. Graphene-engineered automated sprayed mesoscopic structure for perovskite device scaling-up. 2D Materials. 2018;**5**(4):045034. Available from: http://stacks.iop.org/2053-1583/5/i=4/a=045034?key=crossref.2b5fac3fb2b987e29999f38b0cdf07d2

[70] Nia NY, Matteocci F, Cina L, Di Carlo A. High-efficiency perovskite solar cell based on poly(3-hexylthiophene): Influence of molecular weight and mesoscopic scaffold layer. ChemSusChem. 2017;**10**(19):3854-3860. DOI: 10.1002/cssc.201700635

[71] Yaghubinia M, Ebnali M, Mahmoud Zendehdel MY. Improvement of perovskite solar cells photovoltaic performance by localized surface plasmon effect of silver-alumina core-shell nanoparticles. 4th International Conference on Photonics, Optics and Laser Technology (PHOTOPTICS), In: Photoptics. IEEE; 2016. pp. 1-3. Available from: https://ieeexplore.ieee.org/abstract/document/7951303

[72] Song J, Zheng E, Liu L, Wang X-F, Chen G, Tian W, et al. Magnesium-doped zinc oxide as electron selective contact layers for efficient perovskite solar cells. ChemSusChem. 2016;**9**(18):2640-2647. DOI: 10.1002/cssc.201600860

[73] Liu Q, Qin M-C, Ke W-J, Zheng X-L, Chen Z, Qin P-L, et al. Enhanced stability of perovskite solar cells with low-temperature hydrothermally grown SnO_2 electron transport layers. Advanced Functional Materials. 2016;**26**(33):6069-6075. DOI: 10.1002/adfm.201600910

[74] Sardashti MK, Zendehdel M, Nia NY, Karimian D, Sheikhi M. High efficiency $MAPbI_3$ perovskite solar cell using a pure thin film of polyoxometalate as scaffold layer. ChemSusChem. 2017;**10**(19):3773-3779

[75] Gong J, Darling SB, You F. Perovskite photovoltaics: Life-cycle assessment of energy and environmental impacts. Energy & Environmental Science. 2015;**8**(7):1953-1968.

Available from: http://xlink.rsc.org/?DOI=C5EE00615E

[76] Celik I, Song Z, Cimaroli AJ, Yan Y, Heben MJ, Apul D. Life cycle assessment (LCA) of perovskite PV cells projected from lab to fab. Solar Energy Materials & Solar Cells. 2016;**156**:157-169. Available from: https://www.sciencedirect.com/science/article/pii/S0927024816300605?via%3Dihub

[77] Krebs FC, Espinosa N, Hösel M, Søndergaard RR, Jørgensen M. 25th Anniversary article: Rise to power—OPV-based solar parks. Advanced Materials. 2014;**26**(1):29-39. DOI: 10.1002/adma.201302031

[78] Yoo YG, Park J, Umh HN, Lee SY, Bae S, Kim YH, et al. Evaluating the environmental impact of the lead species in perovskite solar cells via environmental-fate modeling. Journal of Industrial and Engineering Chemistry. 2019;**70**:453-461. Available from: https://www.sciencedirect.com/science/article/pii/S1226086X1831339X